CHAPTER III

METHODOLOGY

This chapter presents the experimental set up to study the polarization curve of metals, characteristics of electrochemical reactor used including classical reactor and modified reactor, description of studied conditions, chemical substances, and operating conditions.

1. Experimental set up of polarization curve

Polarization or current density-potential curves of heavy metals were studied to know the individual oxidation - reduction behaviour of each metal. Two procedures were performed in this experiment.

1.1 Potentiostat technique

For this technique, a three electrodes cell was used. The three electrodes consisted of working electrode (W.E.), counter electrode (C.E.) and reference electrode (R.E.) were installed and linked with potentiostat (Model 273 EG&G Princeton Applied Research) as shown in Figure III.1.

A rotating electrode, connecting with platinum disk with speed around 1000 rpm, was used as working electrode. The counter electrode was made of platinum with 1,191 mm^2 in surface area and the reference electrode was saturated calomel electrode. Before starting experiment, about 15 - 20 minutes of nitrogen gas was passed through the solution in order to reduce the oxygen content. The experimental potential was ranging from +2,000 mV/SCE to -2,000 mV/SCE with sweep rate of 5 mV/s. The results showed the curve between current density, oxidation and reduction potential of active species in solution. The curve could be divided into three sections. At the beginning, the starting potential equalled to the standard potential of working electrode. After, the potential was then decreased until the reduction of solution occurred. The last section was the increasing of potential to the anodic zone and the oxidation reaction occurred simultaneously.
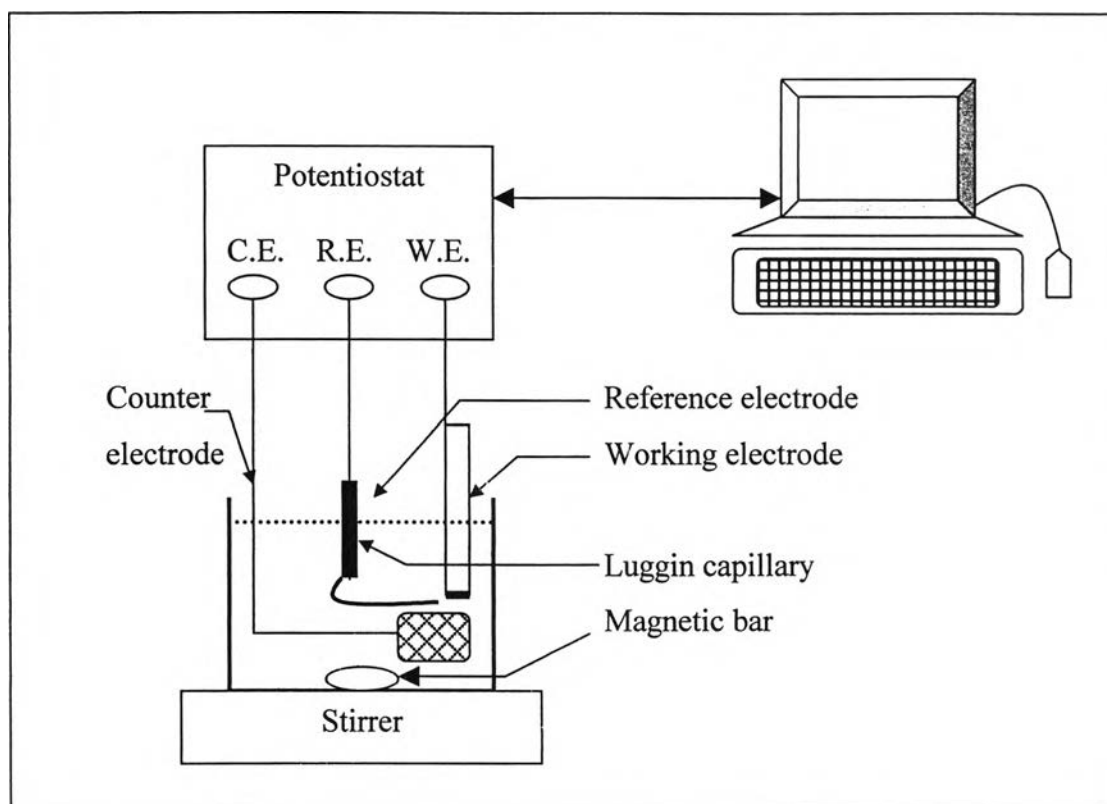
Figure III.1: Schematic diagram of apparatus for current density - potential studies.

1.2 Microbalance technique

The electrochemical quartz crystal microbalance (EQCM) is a very sensitive probe allowing in situ measurements of mass changes occurring during an electrochemical process and resulting generally from the formation or the dissolution of a superficial film [49].

The electrochemical quartz crystal microbalance is experimentally calibrated by measuring the shift of resonance frequency versus the mass change of the active electrode as deduced from the Faraday's law during the cathodic deposition of metal from the solution.

Figure III.2 shows the schematic diagram of the microbalance set up. It is composed of an quartz crystal which is fastened to a submerged impinging jet cell in such a way that the working electrode is uniformly accessible to mass transport. The solution was delivered from the storage tank by a precision gear pump powered by D.C. motor. The platinum grid was used as counter electrode. The working electrode was the gold electrode located on the upper face of quartz crystal disk having 5 MHz

fundamental frequency. It had an approximated active area around 137 mm^2. The potential of working electrode was monitored by a potentiostat against the saturated calomel electrode (reference electrode).
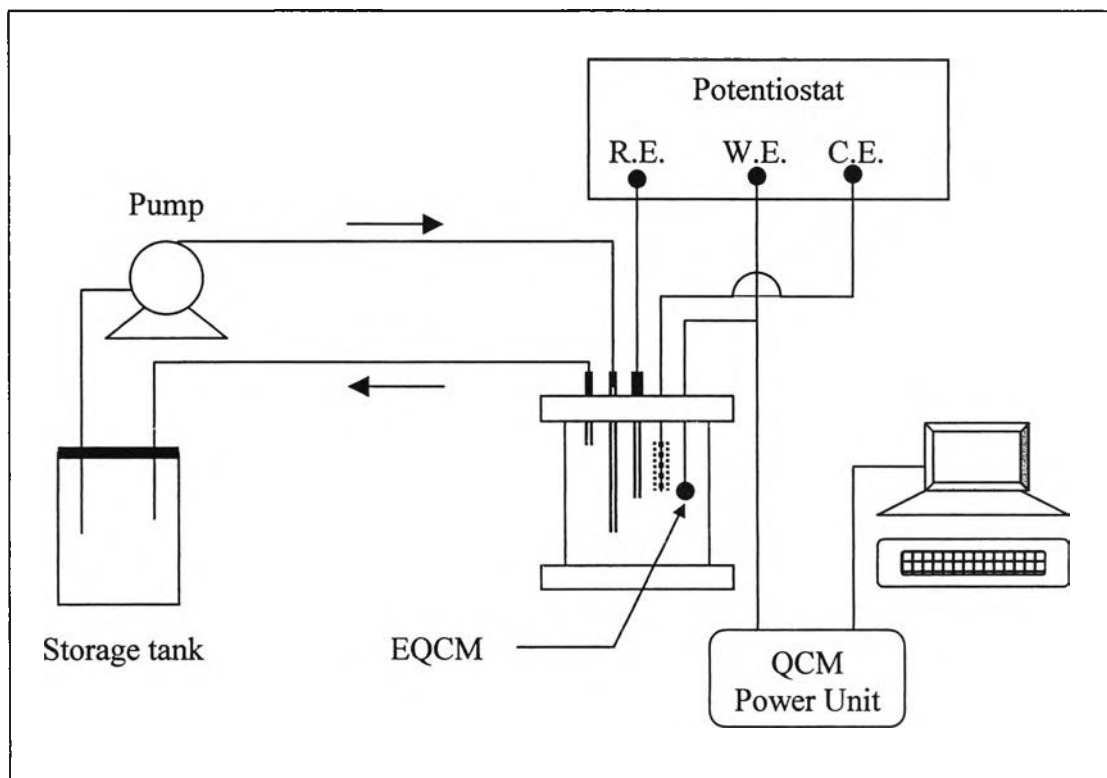

Figure III.2: Scheme of the microbalance set up.

2. Electrolysis of heavy metal

2.1 Description of experimental apparatus

Three types of experimental reactor was used to recover heavy metals from electroplating effluent. They were classical reactor with and without membrane, and the modified reactor (3PE). All experiments were carried out at ambient temperature (25 °C).

2.1.1 Classical reactor without membrane or electrodeposition reactor

Figure III.3 shows the experimental set up of reactor without membrane. This reactor is used to recover copper and zinc by electrodeposition technique.
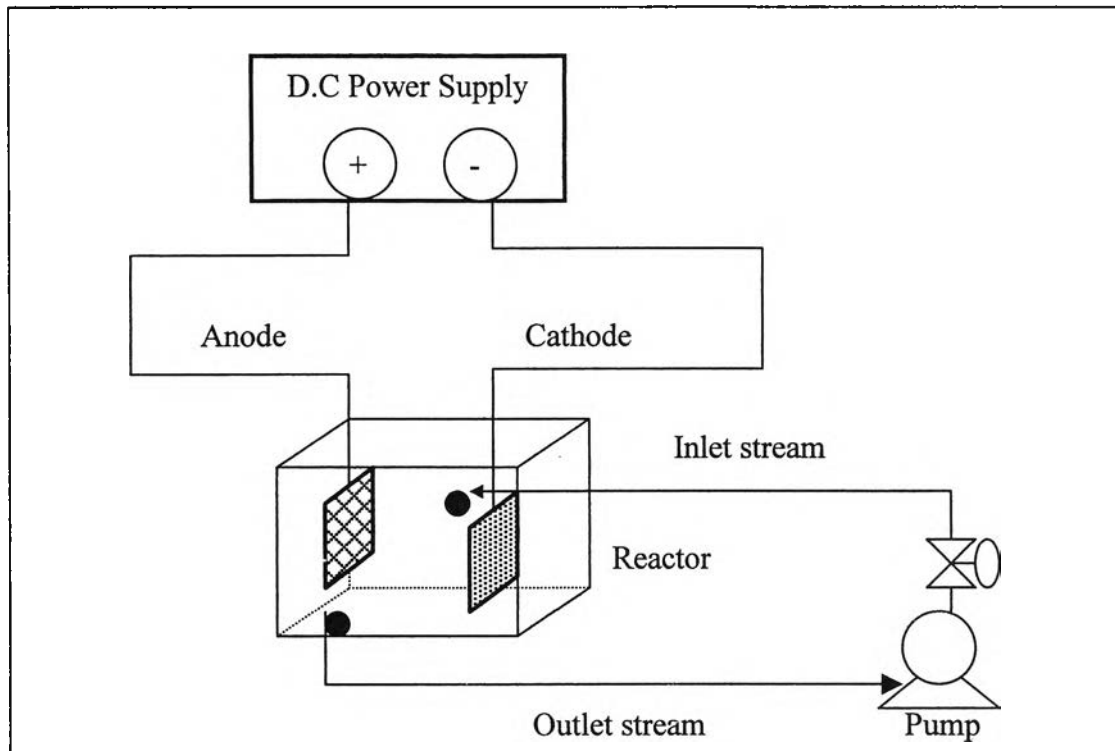
Figure III.3: Schematic view of classical reactor without membrane.

This reactor is consisted of

- Batch reactor (as shown in Figure III.4)

- Size 0.09 m × 0.10 m × 0.08 m

- Cross - sectional area of reactor (A_R) 8 × 10^{-3} m^2

- Hydraulic diameter (d_h) 0.0684 m

- Volume of solution (in reactor and pump) 0.09 m × 0.10 m × 0.11 m

≈ 1 liter

- Pump: Bellow pump type Model 2KB-2X

- Regulated D.C. power supply: type ZS 3205 (0 - 32 VDC; 0 - 5 A)

- Cathode:

Copper recovery

- Stainless steel sheet with surface area 163.6 × 10^{-4} m^2

- Gap inter - electrode (h) 0.052 m

- Dimension of cathode, $L \times l \times t$, 0.08 m × 0.10 m × 0.001 m

(Both sides of cathode are available)

- Holes number (n) 741 holes

- Diameter (*f*) 0.002 m

- Thickness (*t*) 0.001 m

- Specific area of cathode (a_e')14.3 m^{-1}

Zinc recovery

- Zinc plate with surface area 82 × 10^{-4} m^2.

- Gap inter - electrode (*h*) 0.052 m

- Dimension of cathode, *L* × *l* × *t*, 0.082m × 0.1m × 0.001 m

(One side of cathode is accessible)

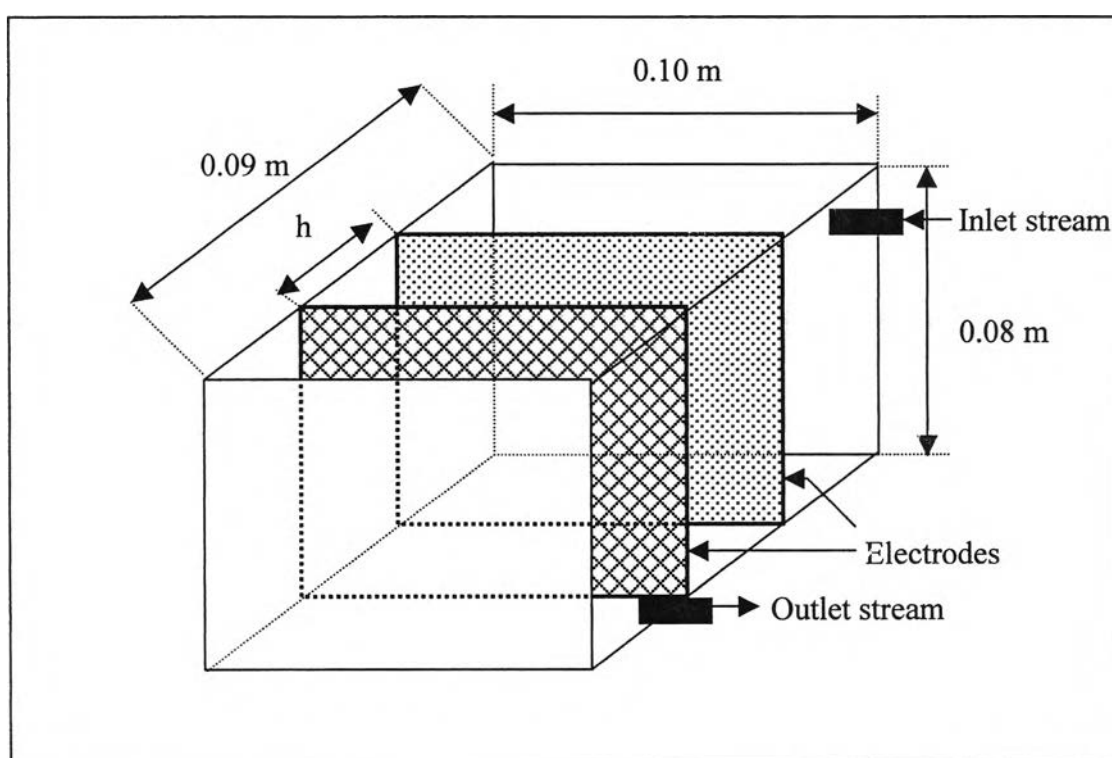- Anode: Titanium grid coated by ruthenium oxide

Figure III. 4: Schematic presentation of electrodeposition reactor.

2.1.2 Classical reactor with membrane or electroprecipitation reactor

The experimental set up is presented in Figure III.5. The system is composed of the following equipments

- Reactor size 0.09 m × 0.10 m × 0.11 m

- Total volume of solution (in reactor and pump) 1 liter

- Two bellow pump type Model 2KB - 2X

- Regulated D.C. power supply: type ZS 3205 (0 - 32 VDC; 0 - 5 A)

- Cathode: stainless steel with surface area 111.5×10^{-4} m^2

- Dimension of cathode, $L \times l \times t$, 0.088 m $\times$ 0.088 m $\times$ 0.001 m

  (Both sides of cathode are available)

- Hole number (n) 49 square - holes

- Dimension of square - holes (f) 0.008 m

- Anode: Titanium grid coated by ruthenium oxide
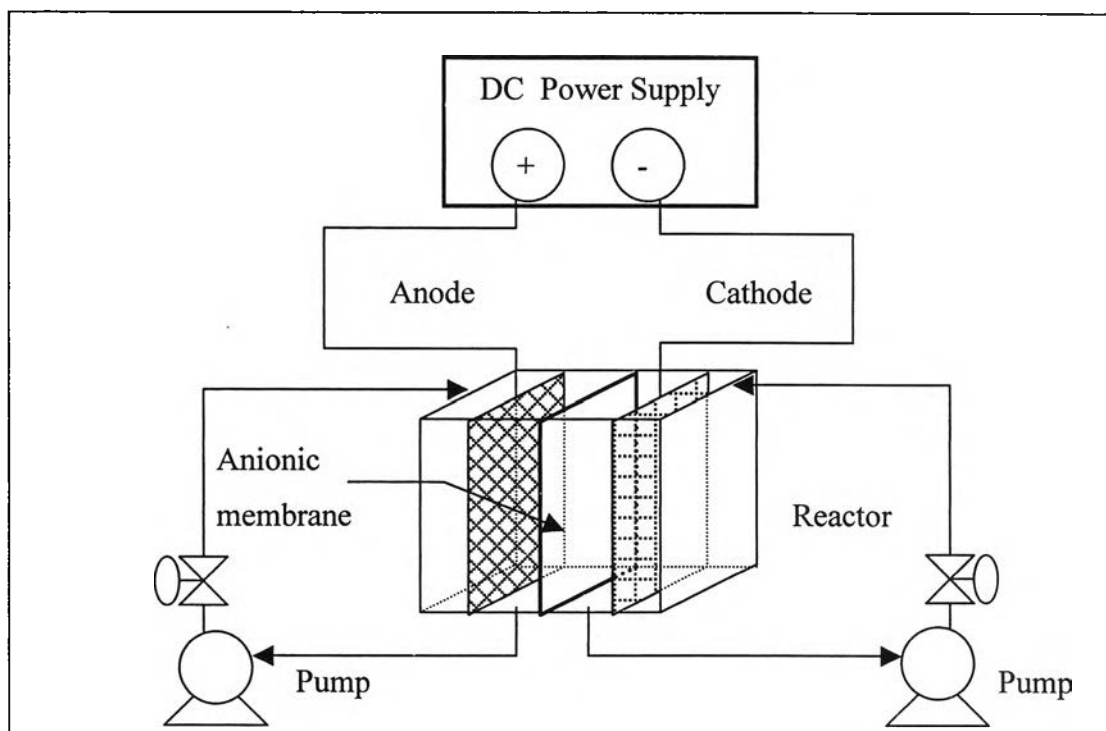
- Anionic membrane type IONAC

Figure III.5: Schematic view of classical reactor with membrane.

2.1.3 Pulsed Porous Percolated Electrode reactor or 3PE reactor

Figure III.6 shows the experimental set up of copper recovery in 3PE reactor. The principle components are composed of

- Reactor

- Axial field configuration

- Diameter 0.2 m

- Height 0.35 m

- Total volume of solution (in reactor + storage tank) 15 liters

- Pump: Magnet pump, type Model MD - 20R

- Regulated D.C. power supply: type PTN 0 - 40 A, 0 - 32 V.

- Cathode: Graphite particle

- Anode: Titanium coated with ruthenium oxide grid

- Current feeder: Stainless steel sheet

1. Anode   2. 3PE reactor   3. Current feeder   4. Electrolyte   5. Particle bed
6. Distributor   7. Diaphragm   8. Motor   9. Reducer   10. Connecting - rod
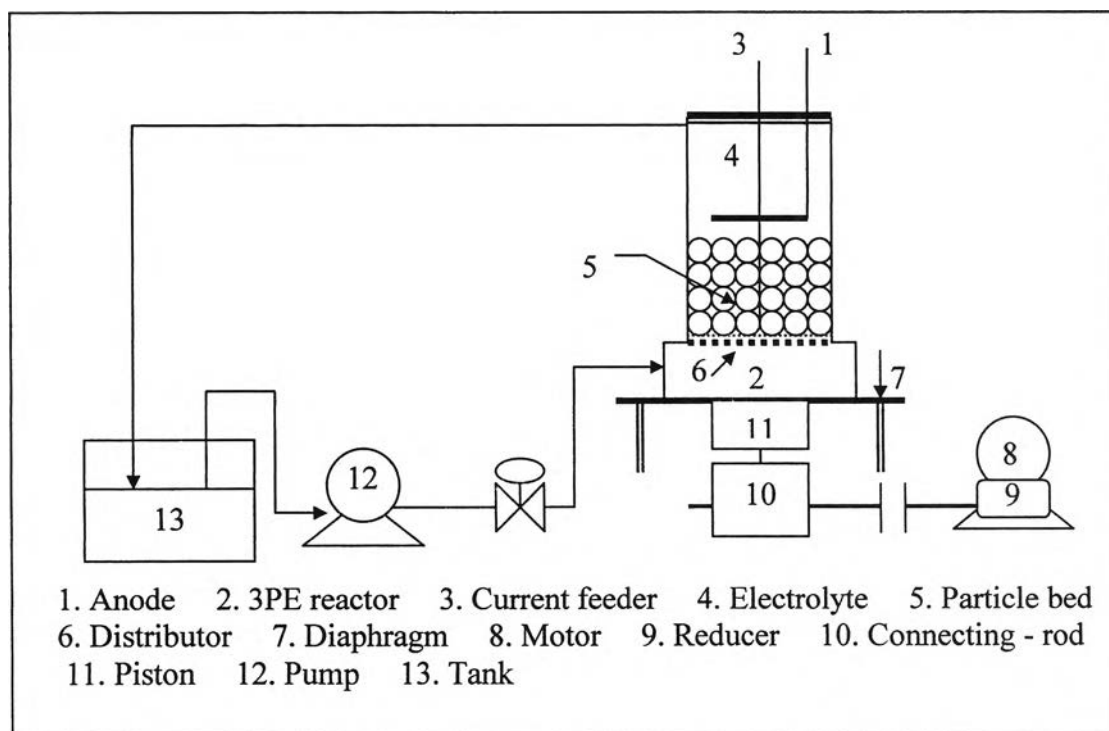11. Piston   12. Pump   13. Tank

Figure III.6: Schematic presentation of 3PE reactor.

Anode was placed above the upper level of particles by about 0.04 - 0.05 m to keep the cell voltage within the range of power supply. The pulsation of the system was conducted by an automatic controller of air (apparatus number 8 - 11 in Figure III.6). The operation of this controller was similar to a sinusoidal wave. The physical properties of electrolyte were obtained from Handbook of Electrolyte solution; Part A at 25 °C [50]. Table III.1 demonstrates the electrode characteristics.

Table III.1: Characteristic of graphite particles used in 3PE reactor.

Graphite particles	
Specific surface area (m^2/m^3)	1000
Total weight (kg)	0.5
Density (kg/m^3)	1069
Total volume of graphite (m^3)	2.96×10^{-4}
Diameter (m)	0.0035

2.2 Chemical substances

The synthetic solutions of each heavy metal and other chemical substances were prepared from the following reagents:

- Copper (II) sulphate ($CuSO_4 \cdot 5H_2O$) with 99% purity

- Chromium (III) potassium sulphate ($CrK(SO_4)_2 \cdot 12H_2O$) with 98% purity

- Nickel (II) sulphate ($NiSO_4 \cdot 6H_2O$) with 98% purity

- Zinc sulphate ($ZnSO_4 \cdot 7H_2O$) with 98 % purity

- Sodium sulphate (Na_2SO_4) with 99 % purity

- Sodium hydroxide (NaOH) with 99 % purity

- Sulphuric acid (H_2SO_4) with 67 % purity

2.3 Description of solutions

The different types of solutions used in this experiment are presented in Table III.2. Concentrations of synthetic solutions prepared for this study were higher than average concentrations obtained from various electroplating industries in order to ensure that all experiment can be applied to the electroplating effluent.

The pH of solution was adjusted by H_2SO_4 until pH equal to 1. For solutions with their pH values equal to 4.6 or 5, NaOH was added to adjust pH solution. 5% by weight of Na_2SO_4 was used to increase conductivity of these solutions in the range of 20 - 40 mS/cm. Two concentrations of copper, 1 and 5 g/l, were investigated. For chromium and nickel, concentrations of each metal were 1 and 10 g/l. In case of zinc,

1 g/l concentration was chosen. Metal concentrations in solution were determined by using Atomic Absorption Spectrophotometer (type AA - 275 Varian).

Table III.2: Characteristics of solutions in experimental studies.

NO.	Types of solutions	Origin	Designated as
1.	Solvent pH = 1 ($H_2O + H_2SO_4$)	Synthetic	SOL 1
2.	Solvent pH = 5 ($H_2O + Na_2SO_4 + NaOH$)	Synthetic	SOL 2
3.	Single copper solution 1 g/l, pH = 1	Synthetic	S1
4.	Single copper solution 1 g/l, pH = 5	Synthetic	S2
5.	Single copper solution 5 g/l, pH = 1	Synthetic	S3
6.	Single chromium solution 1 g/l, pH = 1	Synthetic	S4
7.	Single chromium solution 1 g/l, pH = 4.6	Synthetic	S5
8.	Single chromium solution 10 g/l, pH = 1	Synthetic	S6
9.	Single chromium solution 10 g/l, pH = 4.6	Synthetic	S7
10.	Single nickel solution 1 g/l, pH = 1	Synthetic	S8
11.	Single nickel solution 1 g/l, pH = 5	Synthetic	S9
11.	Single nickel solution 10 g/l, pH = 1	Synthetic	S10
12.	Single nickel solution 10 g/l, pH = 5	Synthetic	S11
13.	Single zinc solution 1 g/l, pH = 1	Synthetic	S12
14.	Mixed solution of Cr, Ni, Zn 1 g/l (for each metal), pH = 1	Synthetic	S13
15.	Mixed solution of Cu, Cr, Ni, Zn 1 g/l (for each metal), pH = 1	Synthetic	S14
16.	Electroplating effluents		
	- Plant I solution	Effluent	S15
	- Plant II solution	Effluent	S16

2.4 Description of operating conditions

Tables III.3 and III.4 show the investigated conditions for individual metal recovery and mixed solutions of metals in a reactor with and without membrane. A reactor for metal recovery was selected depending upon the technique applied. The

electrodeposition reaction was studied with a reactor without membrane whereas the eletroprecipitation reaction was performed with a reactor with membrane.

Table III.3: Operating conditions for metal recovery in a reactor without membrane.

Types of solutions	Operating conditions
Copper solution	
In a classical reactor	
Initial concentration (g/l)	1 and 5
Initial pH	1 and 5
Current density (A/m^2)	5, 10, 15, 17.5, 20, and 25 for 1 g/l
	20, 25, 30, 35, and 40 for 5 g/l
Time (hr)	0 - 11
Flow rate (l/min)	0.42 - 4
In a 3PE reactor	
Initial concentration (g/l)	1
Initial pH	1
Current intensity (A)	5, 6, 7, 9, and 11
Time (hr)	0 - 24
Flow rate (l/min)	3 - 8
Pulse frequency (Hz)	0.16 - 0.43
Zinc solution	
Initial concentration (g/l)	1
Initial pH	1
Current density (A/m^2)	25.6 - 122
Flow rate (l/min)	0.42

Table III.4: Operating conditions for metal recovery in a membrane reactor.

Types of solutions	Operating conditions
Chromium solution	
Initial concentration (g/l)	1 and 10
Initial pH	1 and 4.6
Current density (A/m^2)	90, 126, 153, and 203
Flow rate (l/min)	0.42
Nickel solution	
Initial concentration (g/l)	1 and 10
Initial pH	1 and 5
Current density (A/m^2)	90, 126, 153, and 203
Flow rate (l/min)	0.42
Mixed solution of Cu, Ni, Cr, Zn	
Initial concentration(g/l of each metal)	1
Initial pH	1
Current density (A/m^2)	10 for copper
	90 for chromium, nickel and zinc
Flow rate (l/min)	0.42
Electroplating effluents	Similar to the conditions of the above synthetic mixed solution

3. Polarization curves of heavy metal solutions

3.1 Potentiostat technique

The polarization curves or current density - potential curves of metals were investigated to check the possibility of electrochemical metal deposition and to find the working potential range.

3.1.1 Polarization curve of solvents

Figure III.7 shows the current density - potential curve of solvent at pH = 1 (SOL 1) and pH = 5 (SOL 2), the potentials start from +1,500 mV/SCE to -1,500 mV/SCE.

This curve pointed out that the domain of electroactive species was limited by two potentials. The first potential is the reduction potential of water. The second potential is the oxidation potential of water to release oxygen gas. The production of hydrogen gas is observed at potential lower than zero whereas one of oxygen gas is obtained with potential which higher than zero. The reactions for both gases are displayed by

Production of O_2: $\quad 2H_2O \quad \longrightarrow \quad O_2 + 4H^+ + 4e^- \qquad$ (III.1)

Production of H_2: $\quad 2H^+ + 2e^- \longrightarrow \quad H_2 \qquad$ (III.2)
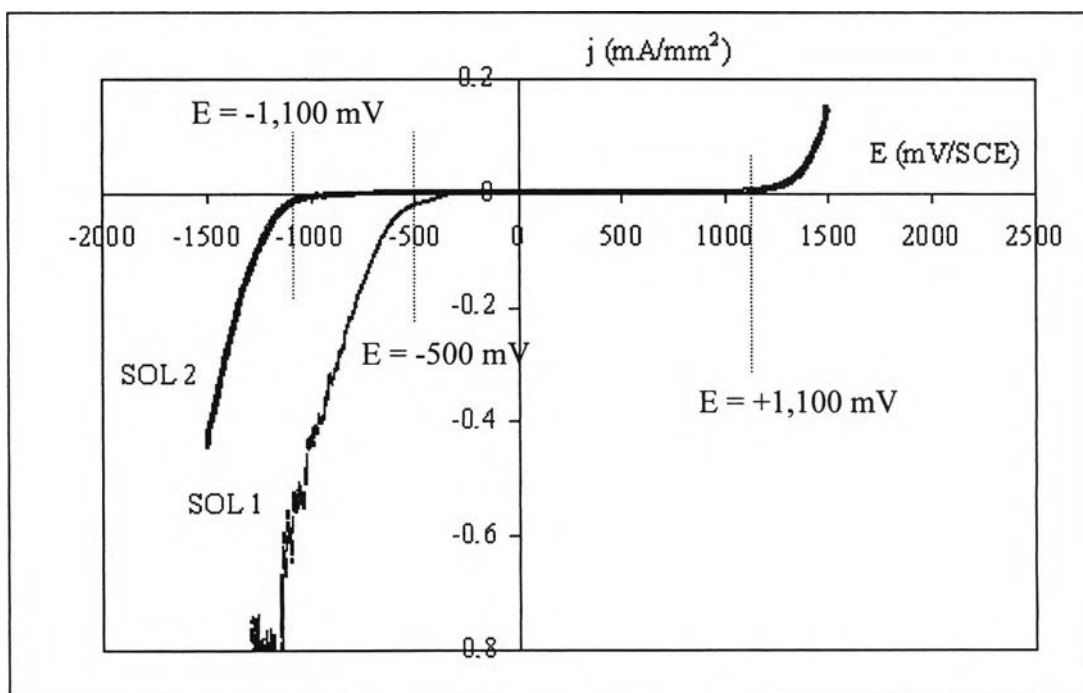
Figure III.7: Polarization curve of solutions SOL 1 and SOL 2.

For solution SOL 1, the domain of potential was valid until being produced hydrogen gas by reduction reaction of water at potential -500 mV/SCE. On the other

hand, in case of solution SOL 2, the reduction of water was observed for potential lower than -1,100 mV/SCE which is corresponding to hydrogen gas evolution. An oxygen gas was observed corresponding to the oxidation reaction of water at potential more than +1,100 mV/SCE. So, it can be said that, the reduction or oxidation potential of water depends upon the pH of that aqueous solution and the type of electrode used. The reduction potential of water or proton of low pH solution is also higher than that of high pH solution.

3.1.2 Polarization curve of synthetic copper solutions

The current density - potential curve of copper solution was emphasised from +1,000 mV/SCE to -1,000 mV/SCE for a concentration of 1 g/l at pH = 1 (solution S1) and the same concentration at pH = 5 (solution S2).
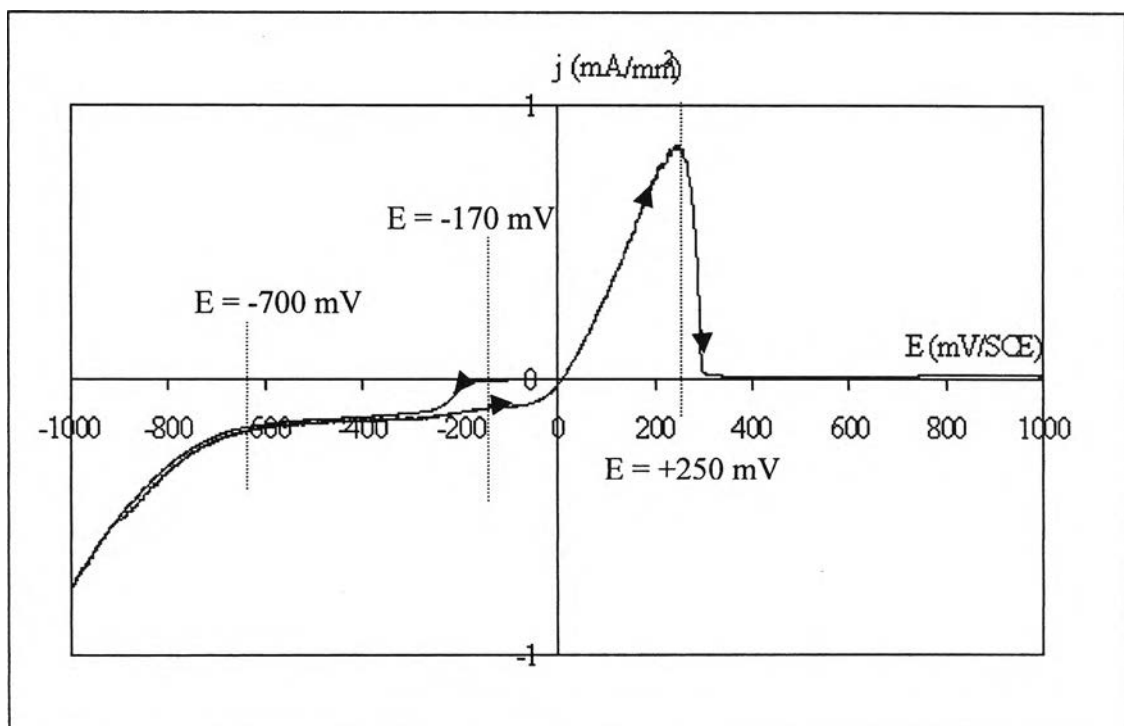
Figure III.8: Polarization curve of solution S1.

The results of the solution S1 are presented in Figure III.8. The reduction of copper started at -170 mV/SCE. The current density suddenly increased until it reached -0.2 mA/mm^2 at -250 mV/SCE and then kept constant until -700 mV/SCE.

During anodic scan, one oxidation peak of copper was observed for potential higher than 0 mV/SCE. The current density rapidly increased to up 0.84 mA/mm^2 at +250 mV/SCE. This peak corresponds to the oxidation of copper which has deposited during the reduction phase.

Figure III.9 shows the current density-potential curve solution S2. The results presented that the reduction of copper was observed for potential lower than -350 mV/SCE and it grew up to -450 mV/SCE. After that, current density was constant until -600 mV/SCE which is corresponding to -0.06 mA/mm^2. Considering the anodic scan, the copper oxidation peak was observed at potential +190 mV/SCE corresponding to 0.91 mA/mm^2 current density.

From the study of both pH, it can conclude that there is a possibility to recover copper by electrodeposition at potential less than -170 mV/SCE and less than -350 mV/SCE for synthetic copper solution at pH = 1 and pH = 5.
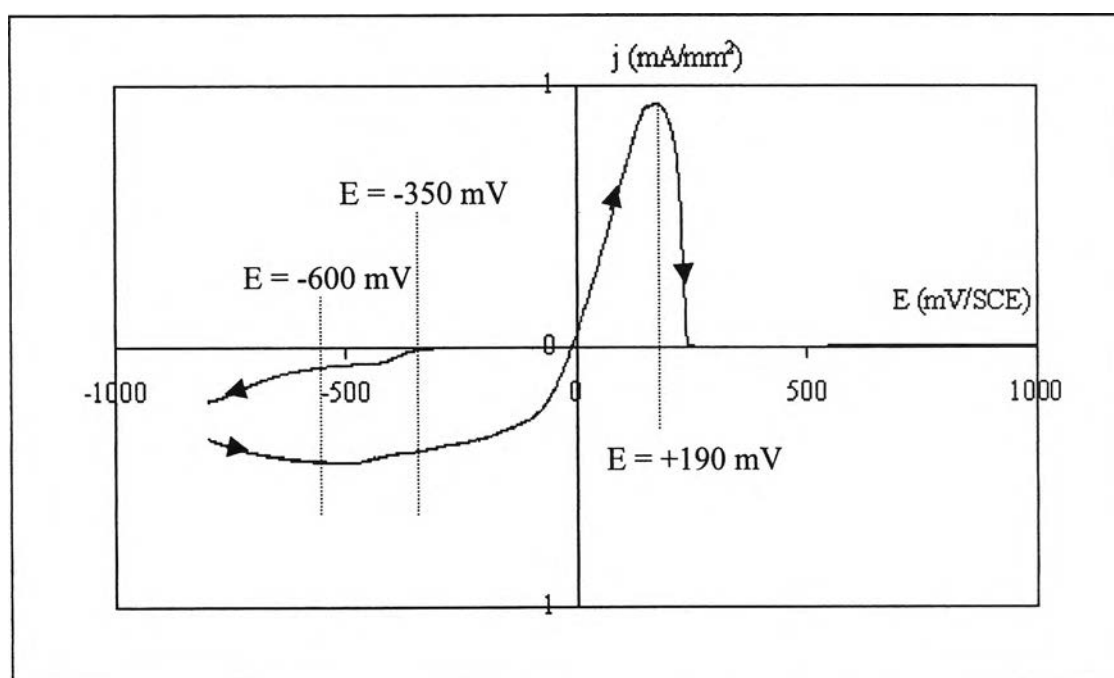

Figure III.9 Polarization curve of solution S2.

3.1.3 Polarization curve of synthetic chromium solutions

The polarization curve of chromium was investigated by using 1 g/l of synthetic solution at pH = 1 (solution S4) and the same concentration at pH = 4.6 (solution S5).

The potential for solution S4 was started in a range from +500 mV/SCE to -1,000 mV/SCE as shown in Figure III.10. The changing of current density was observed at potential lower than -300 mV/SCE. This results from the reduction of proton to hydrogen gas. The reduction peak of chromium was not observed in this case. When the cathodic potential was much lower, fluctuation of curve was strongly observed because the large amount of hydrogen gas was produced.
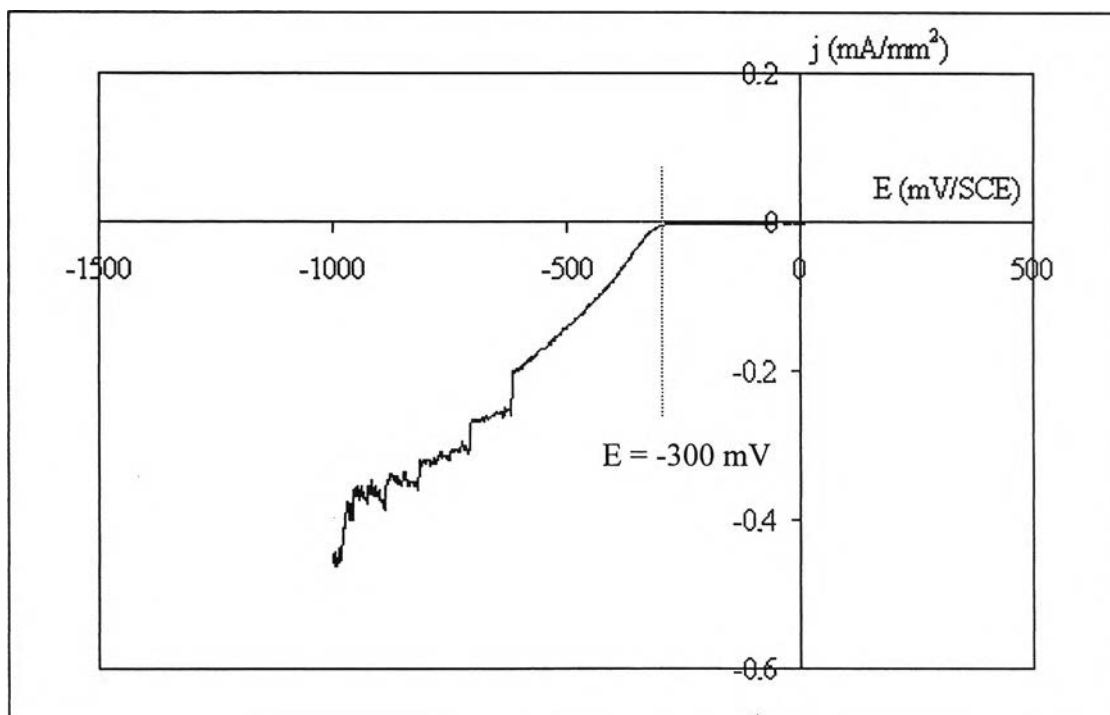

Figure III.10 Polarization curve of solution S4.

Figure III.11 demonstrates the current density - potential curve of solution S5 in potential ranging from +1,000 mV/SCE to -1,800 mV/SCE. The results showed that a little reduction wave was observed in a period of cathodic scan from -700 mV/SCE to -1,100 mV/SCE. This wave may be corresponding certainly to the reduction of chromium (III) to chromium (II).

In actual operation, it is difficult to recover chromium by deposition on cathode surface because of its own operating limitations. It needs specific operating conditions and specific initial pH. Moreover, the chromium contained in electroplating effluent is generally found in hexavalent form (Cr^{6+}) which is inefficient to remove by electrodeposition technique. This phenomenon attracts the

author to apply an electroprecipitation technique to recover chromium instead of electrodeposition technique.
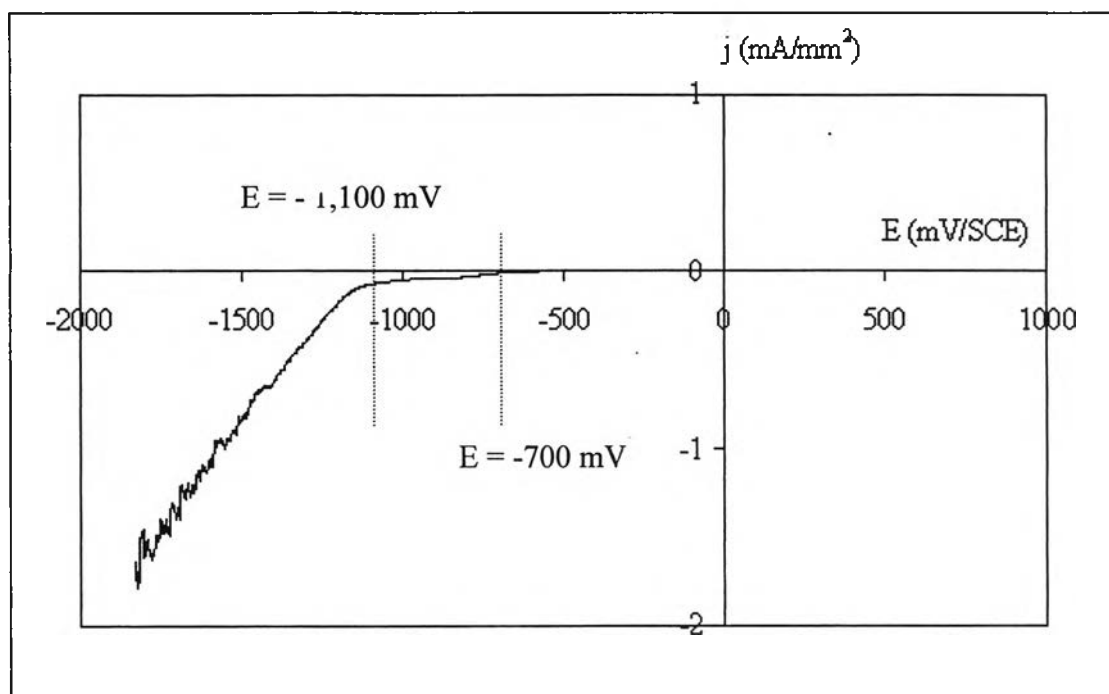

Figure III.11: Polarization curve of solution S5.

3.1.4 Polarization curve of synthetic nickel solutions

Synthetic nickel solution with 1 g/l concentration was prepared and pH was adjusted to 1 (solution S8) and 5 (solution S9) by H_2SO_4 and NaOH.

Figure III.12 presents the current density - potential curve of solution S8. The studied potential was ranging from +500 mV/SCE to -800 mV/SCE. The result indicated that the reduction wave of nickel was less easily observed because the nickel reduction potential occurred at a potential close to the reduction potential of proton. In anodic direction, the oxidation of nickel to nickel ions was weakly observed. Figure III.13 reviews the current density - potential curve of solution S9. The reduction reaction was slightly observed at potential about -700 mV/SCE and the oxidation peak was small observed in anodic direction.

From this study, nickel reduction is also difficult for both low and high initial pH solution so the precipitation technique is carried out to remove nickel from solutions.
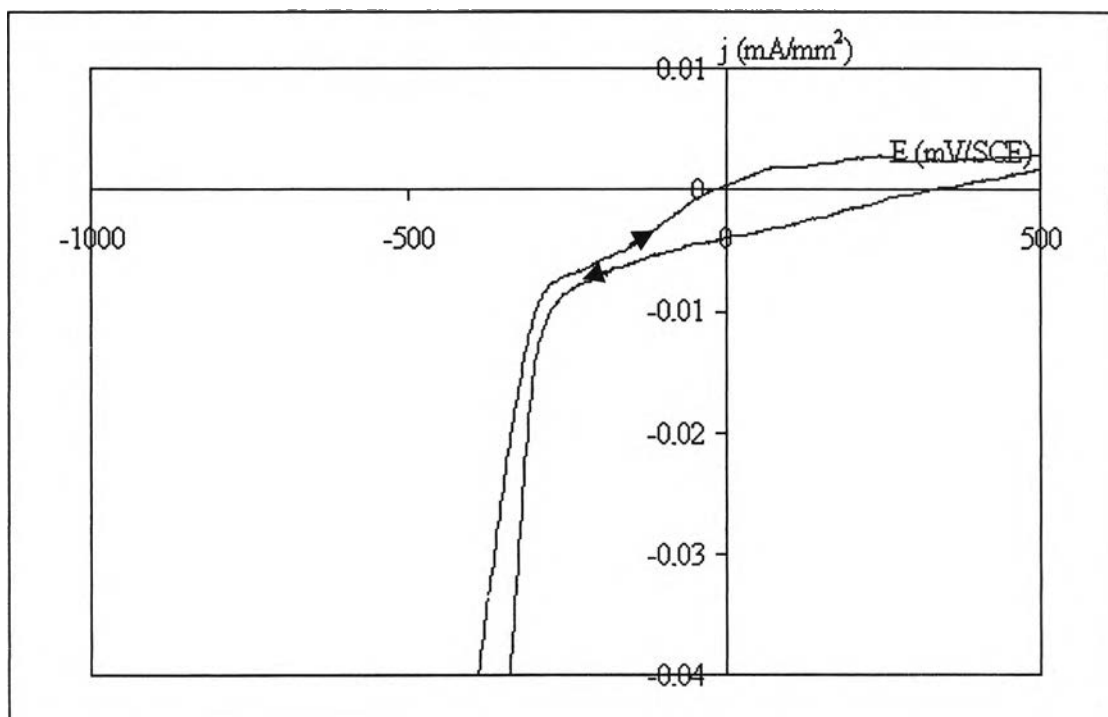
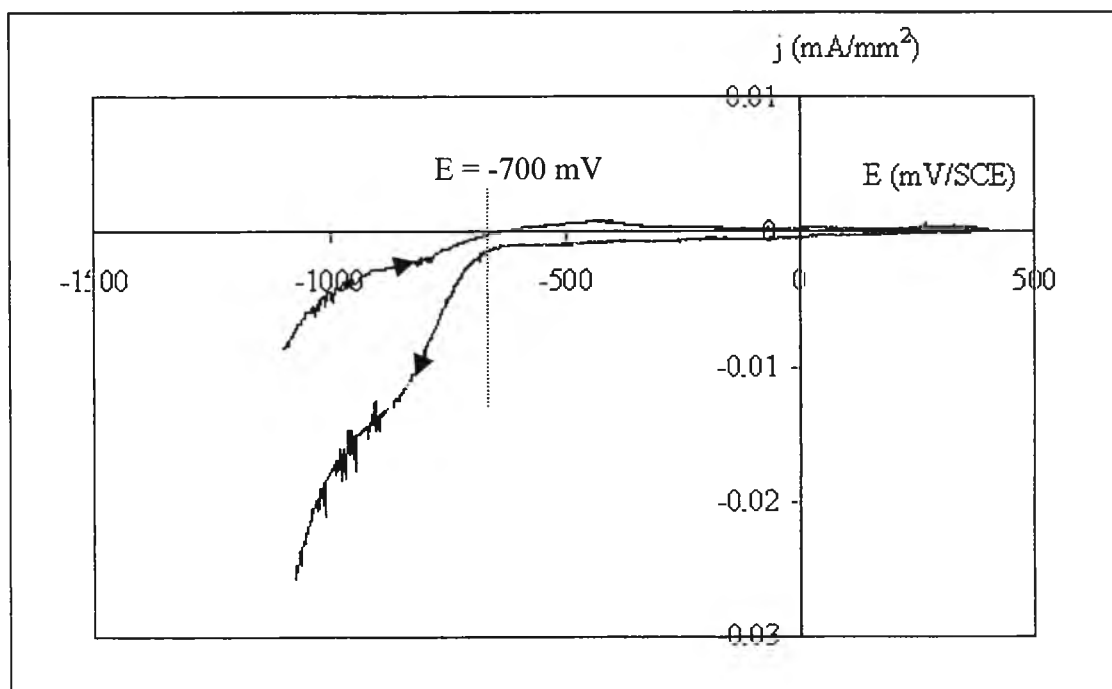Figure III.12: Polarization curve of solution S8.

Figure III.13: Polarization curve of solution S9.

3.1.5 Polarization curve of synthetic zinc solutions

For 1 g/l of synthetic zinc concentration at pH = 1 (solution S12), the polarization curve was studied from 0 mV/SCE to -1,800 mV/SCE. Nitrogen gas was passed through the solution about 15 minutes before starting the experiment to decrease the amount of oxygen in solution. Figure III.14 shows the current density - potential curve of solution S12. The absolute value of the current increased at potential about -350 mV/SCE until it reached A point which a potential equals to -800 mV/SCE. The change of current around A point corresponded to the reduction of solvent on cathode to hydrogen gas as shown in Figure III.15. After passing the A point, the potential of cathode resembles to the reduction of zinc on cathode until reaching -1,300 mv/SCE at B point. The potential after passing the B point corresponded to the reduction potential of proton on cathode which is covered by deposited zinc. During the anodic scan, the oxidation of deposited zinc was strongly observed at potential about -750 mV/SCE corresponding to 0.58 mA/mm^2 current density. From this study, it can be concluded that the potential range for the reduction of synthetic zinc solution at pH = 1 starts from -800 mV/SCE to -1,300 mV/SCE. The best reduction potential of zinc is around the B point because the maximum metal deposition occurs here.
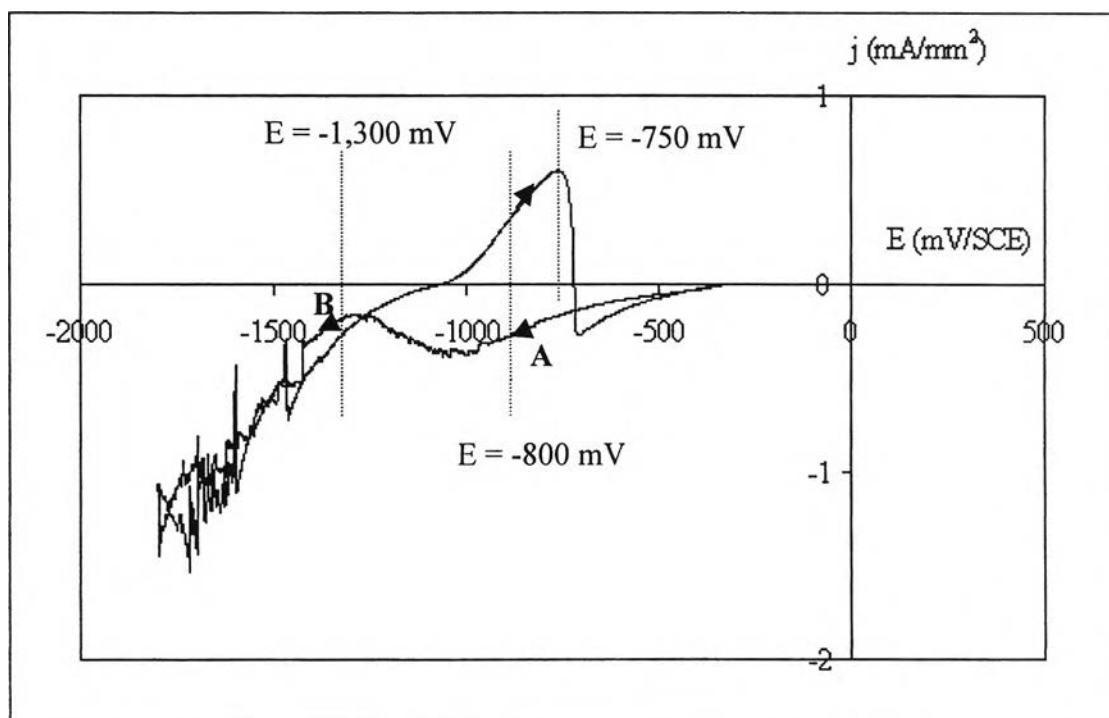

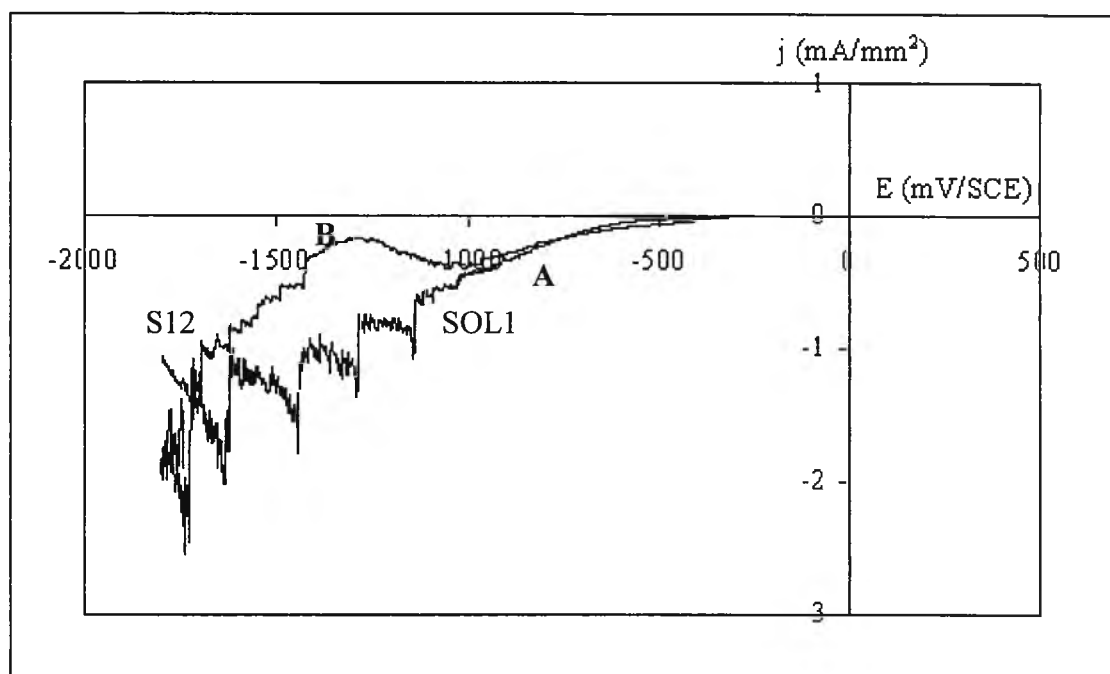Figure III.14: Polarization curve of solution S12.

Figure III.15: Comparison between polarization curve of solutions SOL 1 and S12.

3.1.6 Polarization of synthetic mixed solution of copper, chromium, nickel and zinc

The current density - potential curve for mixed solution of copper, chromium, nickel and zinc (solution S14) was investigated at potentials from +1,000 mV/SCE to -1,500 mV/SCE. The pH of this synthetic solution was about 1. The result is shown in Figure III.16. It indicated that a reduction wave was observed in potential range from -170 mV/SCE to -700 mV/SCE corresponding to cathodic current density of -0.2 mA/mm^2. This wave corresponds to the copper reduction and no appearance of reduction peak of chromium, nickel and zinc.

In the previous current density - potential study of chromium, nickel, and zinc, the reduction of chromium and nickel was not clearly observed and the reduction of zinc was distinct appearance at potential lower than -800 mV/SCE. However, the reduction peak of these three metals was not observed in mixed solution because the reduction chromium and nickel occurs difficultly and the reduction of zinc occurs at more negative potential than this studied potential range.

During the anodic scan, an oxidation peak (1.08 mA/mm^2 current density) was mainly observed at potential about +360 mV/SCE. It is close to the oxidation peak of copper in single solution. In chromium, nickel, and zinc case, no oxidation peaks were observed here.
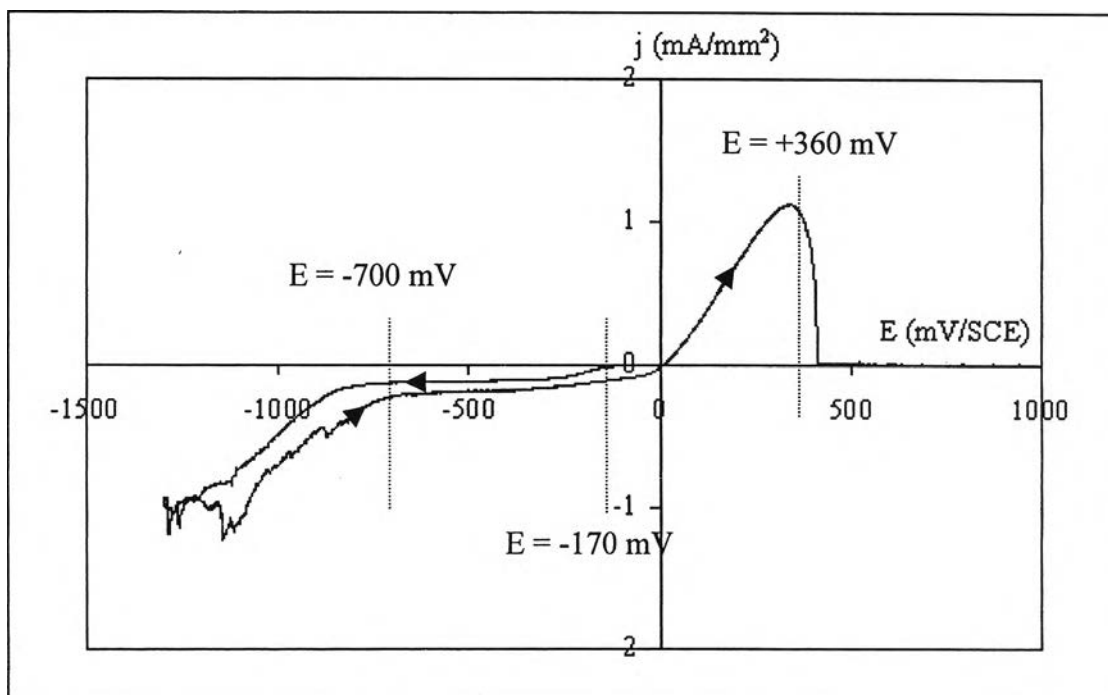

Figure III.16: Polarization curve of solution S14.

3.2 Microbalance technique

Due to the limitation of the potentiostat technique, it does not give good evidence of polarization curve of some metals such as nickel, the microbalance technique was then applied for nickel and zinc solution. This technique gives the precise information on metal reduction which observes from the thickness of deposited metal layer and rate of metal deposition (df/dt) as a function of potential monitored by the potentiostat. When the reduction occurs at the beginning of proton reduction, the hydrogen gas does not disturb the system.

This technique was conducted as a complementary technique to analyse the current density - potential curve of nickel and zinc.
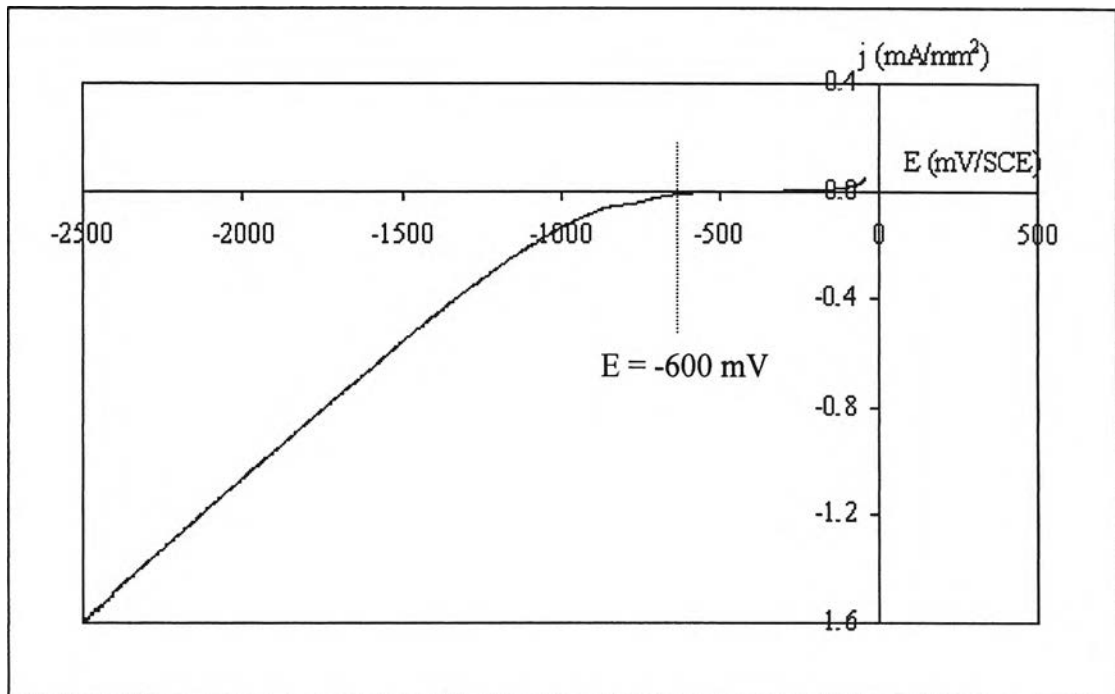
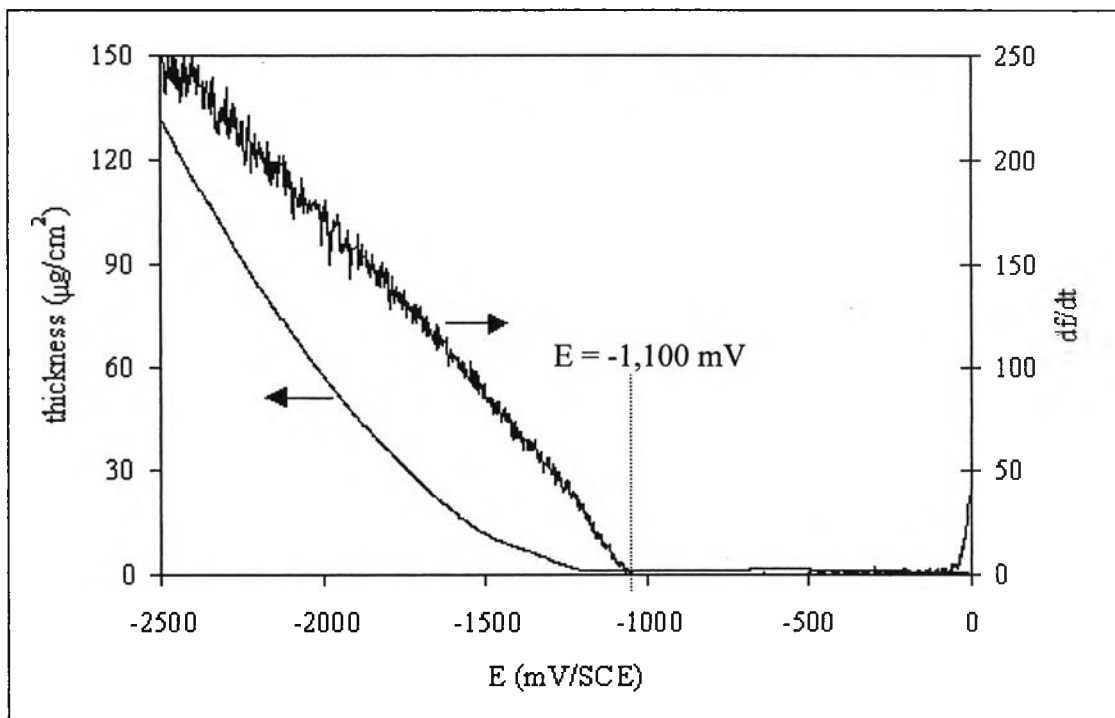Figure III.17: Polarization curve of nickel solution (0.25 g/l, pH = 1).

Figure III.18: Thickness layer and frequency divided by time of nickel deposition
versus potential (0.25 g/l, pH = 1).

Synthetic nickel solution with concentration of 0.25 g/l at pH = 1 was used to perform microbalance technique during potentials of 0 mV/SCE to -2,500 mV/SCE. Figure III.17 shows the current density-potential curve of nickel. The plot indicated that nickel began to deposit at -600 mV/SCE and followed by the reduction of water or proton to hydrogen gas. However, comparing with the results indicated in Figure III.18, which presents the plot of thickness deposited layer and metal deposition rate, it showed that the rate of nickel deposition began to change at potential about -1,100 mV/SCE. So, it means that nickel starts to deposit at potential around -1,100 mV/SCE. It indicated that, at potential -600 mV/SCE, the reduction of nickel does not happen. The conversion of cathodic current may come from the reduction of the solvent of the system. The exact reduction potential was observed by the increasing of the deposited metal layer thickness. From this study, it can be concluded that the reduction reaction of nickel occurred at -1,100 mV/SCE.

For zinc case, the solution was synthesized at 0.25 g/l concentration and pH = 1. The solution was studied at potential ranging from +500 mV/SCE to -2,000 mV/SCE by microbalance technique.
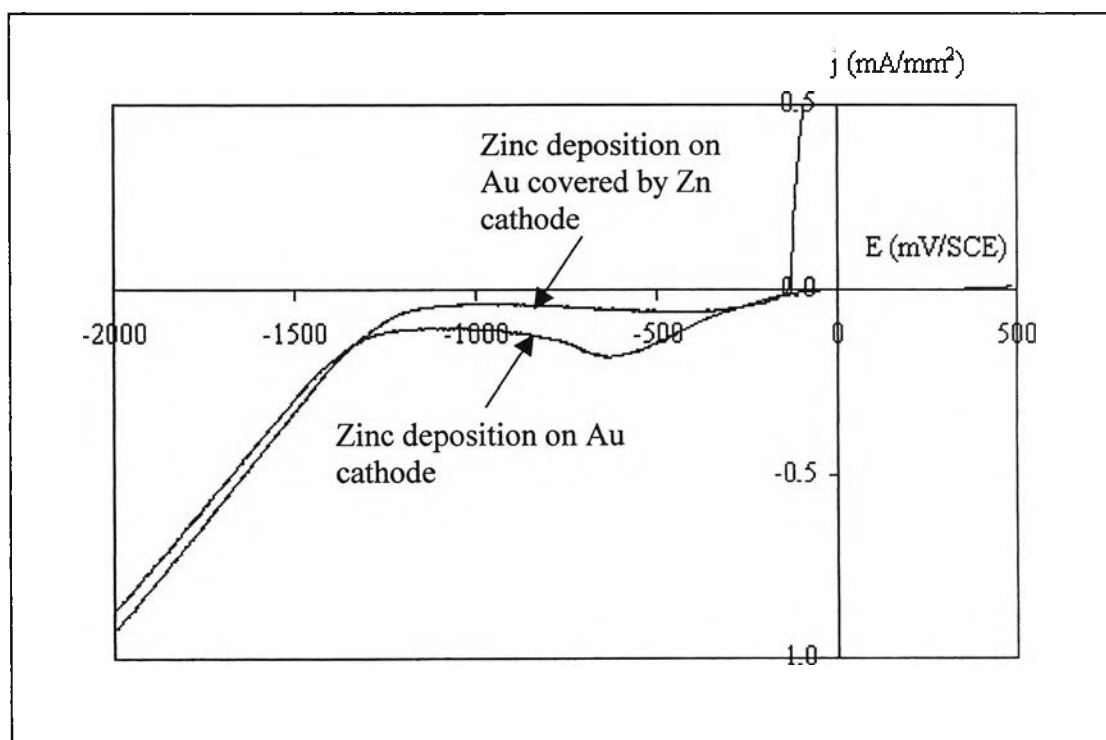

Figure III.19: Polarization curve of zinc solution (0.25 g/l and pH = 1).

Figure III.19 shows current density - potential curve of zinc on gold cathode and on gold cathode covered by zinc. It showed that the tendency of current density - potential line had a difference in that the maximum production of proton observed on gold cathode was found at potential around -500 mV/SCE. On the other hand, the same behaviour was not observed on gold covered by zinc. So, it can be said that the current density - potential curve depends upon the cathode used in the process.

Figure III.20 demonstrates the relationship of thickness layer and change in frequency versus time and applied potential. Zinc started to deposit at potential about -900 mV/SCE and the zinc deposition increased rapidly with potential. In addition, the frequency of zinc deposition gave the same behaviour as thickness, it increased when potential increased.
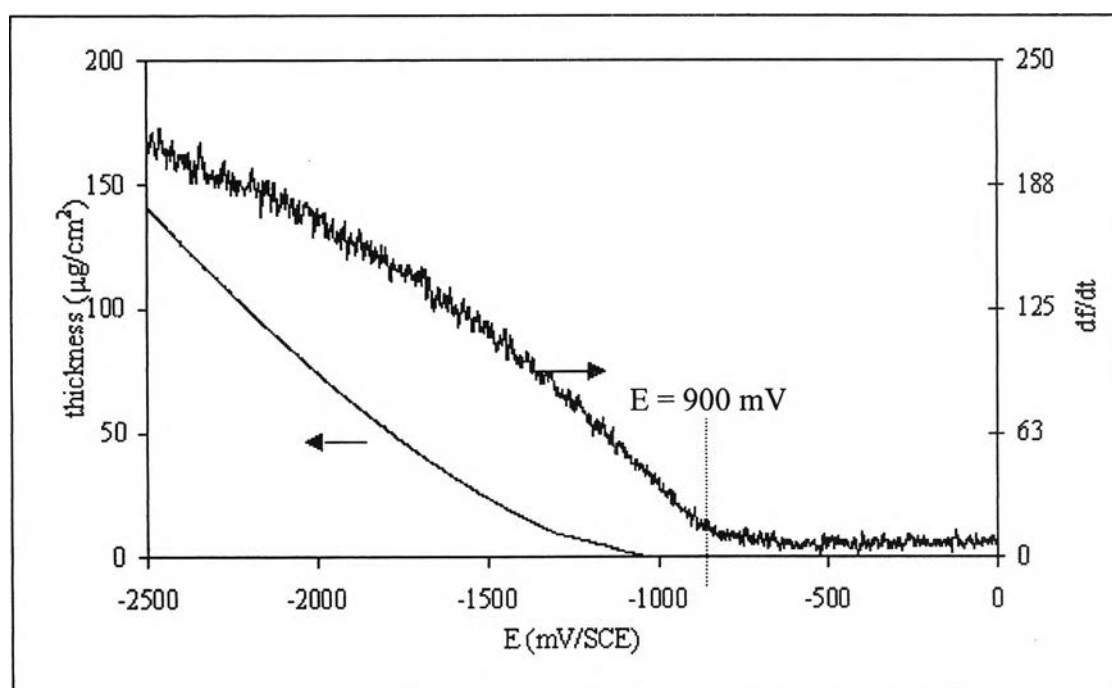

Figure III.20: Thickness layer and frequency divided by time of zinc deposition versus potential (0.25 g/l and pH = 1).

This chapter has displayed the experimental set up of metal recovery from electrolyte solution. Three types of electrochemical reactor with different advantages were used. The suitable reactor for each metal is determined depending upon the possibility of metal reduction which can be observed from the polarization curve.

The current density - potential curves of heavy metals including copper, chromium, nickel, zinc, and mixed solution of them were presented at the last part of this chapter. The reduction of copper and zinc was strongly observed during the interesting potential range. The reductions of copper with concentration of 1 g/l at pH = 1 and pH = 5 were found at potential lower than -170 mV/SCE and -350 mV/SCE, respectively. For zinc, the reduction was observed at potential of -1,300 mV/SCE. In case of chromium and nickel, the reduction was weakly observed due to some limitations. For these reasons, the recovery technique chosen for copper and zinc should be the deposition technique which is carried out in reactor without membrane. On the other hand, for nickel and chromium, the precipitation technique should be preferred in reactor with membrane.